NUCLEAR PHYSICS

Electroexcitation of Low-Lying Particle-Hole RPA States of ^{16}O with WBP Interaction

Commun. Theor. Phys. **62** (2014) 839–846 Vol. 62, No. 6, December 1, 2014

Electroexcitation of Low-Lying Particle-Hole RPA States of ^{16}O with WBP Interaction

Ali H. Taqi,[1,*] R.A. Radhi,[2] and Adil M. Hussein[3]

[1]Department of Physics, College of Science, Kirkuk University, Kirkuk, Iraq

[2]Department of Physics, College of Science, University of Baghdad, Baghdad, Iraq

[3]Department of Physics, College of Science, University of Sulaimani, Sulaimani, Iraq

(Received February 10, 2014; revised manuscript received June 20, 2014)

Abstract *The nuclear structure of ^{16}O is studied in the framework of the particle–hole random phase approximation (ph RPA). The Hamiltonian is diagonalized within a model space with particle orbits $\{1d_{5/2}, 1d_{3/2}$, and $2s_{1/2}\}$ and the hole orbits $\{1p_{3/2}$ and $1p_{1/2}\}$ using Warburton and Brown interaction WBP. The ph RPA calculations are tested, by comparing the electron scattering form factors with the available experimental data. The results of electron scattering form factors and reduced transition strength for the states: 1^-, $T = 0$ (7.116 MeV); 2^-, $T = 1$ (12.968 MeV); 2^-, $T = 1$ (20.412 MeV); and 3^-, $T = 0$ (6.129 MeV) are interpreted in terms of the harmonic-oscillator (HO) wave functions of size parameter b. The occupation probabilities of the single particle and hole orbits are calculated. The spurious states are removed by adding the center of mass (CM) correction to the nuclear Hamiltonian. A comparison with the available experiments data is presented.*

PACS numbers: 21.60.Jz, 21.60.Ev, 13.40.Gp
Key words: random-phase approximation, collective excitations and electromagnetic form factors

1 Introduction

Major challenge in theoretical nuclear physics is the development of a universal approach able to describe the excited states of all nuclear systems with the same accuracy. The problem of a nuclear structure is a many-body problem, as it arises in many branches of physics. In the many-body problem, the dimension of Hilbert space rapidly grows as the particle number increases and the dimension of such space is too large in many cases, preventing us from performing the full calculations. Therefore, the calculations are possible for a truncated model space and various approximate approaches exist to deal with such systems.[1]

The simple shell-model (SM) which is partly analogous to the atomic SM was developed at the beginning of the fifties of the previous century at the time when the nucleon-nucleon potential was not yet well known. It is based on the independent particle approximation, which ignores all correlation effects. It can be used in its simplest single-particle form to provide a qualitative understanding, but it can also be used as a basis for more complex and complete calculations. This model predicts or explains with some success properties of nuclei, in particular spin and parity of nuclei ground states, and to some extent their excited states as well. In nuclear physics, the SM potential is based on empirical facts rather than calculated ones.[2]

Shell-model is based on the mean-field potential also based on the independent particle approximation. The fundamental mean-field theory in the quantum many-body problem is Hartree–Fock (HF) theory which has proved to be a successful method of linking the ground-state properties of nuclei to the nucleon-nucleon interaction. The main idea of mean-field theory (MFT) also known as self-consistent mean-field theory, is approximation for reducing problems of many strongly interacting nucleons to one of non-interacting particles in an average nuclear field.[3]

In the case of closed shell nuclei, the simplest correlation beyond the Hartree–Fock (HF) can only be taken into account by breaking the HF core and raising a nucleon from below to above the Fermi level; then the resulting states must have a particle-hole pair. The excited collective oscillation can be described as a linear combination of particle-hole states. Such an approximation is called the particle-hole Tamm–Dancoff approximation (ph TDA).[4−6] A system of states more general than that considered in the ph TDA appears when treating the ground states and the excited states more symmetrically. In that case, one allows both to have particle-hole pairs. Such an approximation is referred as the particle-hole Random Phase Approximation (ph RPA).[7−10]

Self-consistent HF theory can also be made time-dependent (TDHF) to describe giant resonances and low-lying excited states. TDHF in the limit of linear-response is equivalent to the collective motion model RPA of many-body perturbation theory. Most RPA calculations have been achieved in the matrix diagonalization scheme. Since

*E-mail: alitaqibayati@yahoo.com

the calculation of residual interaction is rather tedious for realistic interaction, it has been common to ignore some terms in practice and to sacrifice the full self-consistency.[11] Recently several groups have reported fully self-consistent RPA and the quasiparticle RPA (QRPA) calculations with Skyrme-type interactions,[12−13] with a modified realistic potential[14] with Gogny force,[15−16] and from solving relativistic mean field equations.[17−18] A more detailed surveys and exhaustive list of references can be found in [19].

Elastic and inelastic electron scattering from atomic nuclei is a successful and powerful tool in investigating the theoretical nuclear models. The interaction between electron and nucleus is an electromagnetic interaction, the theory of which is well established and settled. Thus, in electron scattering experiments one can obtain directly information about the structure of the nucleus. The comparison between the calculated and measured electron scattering form factors has long been used as a successful test of nuclear models.[20−23]

In this work, the structure of ^{16}O is to be studied in the framework of the ph RPA. The calculation within a model space with particle orbits $\{1d_{5/2}, 1d_{3/2}$, and $2s_{1/2}\}$ and the hole orbits $\{1p_{3/2}$ and $1p_{1/2}\}$ using Warburton and Brown interaction WBP[24] is performed. The $1s$, $1p$, $2s1d$, $2p1f$ – shells (WBP) interaction is determined by least square fitting with experimental single particle energies SPE and two-body matrix element TBME. The spurious states are removed by adding the center of mass correction (CMC) to the interaction. The results of electron scattering form factors and reduced transition strength for the states: 1^-, $T = 0$ (7.116 MeV); 2^-, $T = 1$ (12.968 MeV); 2^-, $T = 1$ (20.412 MeV); and 3^-, $T = 0$ (6.129 MeV) are interpreted in terms of the harmonic-oscillator wave functions of size parameter b and effective charges. The occupation probabilities of the single particle and hole orbits are calculated.

2 Theory

2.1 *ph RPA*

If we think of a ground state containing $2p$-$2h$ correlations, the collective excited states of closed shell and sub-shell systems of multipolarity J and isospin T can not only create a ph pair but also destroy one. The quasiboson operator reads[4]

$$Q^{\dagger}_{\omega,JT} = \sum_{mi} [X^{JT}_{mi} a^{\dagger}_m a_i - Y^{JT}_{mi} a^{\dagger}_i a_m] \,, \tag{1}$$

where the label m represents particle states and i is for hole states, the minus sign has been chosen for convenience. The ph RPA ground state is defined via the condition

$$Q_{\omega,JT}|\mathrm{RPA}\rangle = 0 \quad \text{and} \quad Q^{\dagger}_{\omega,JT}|\mathrm{RPA}\rangle = |\omega\rangle \,. \tag{2}$$

In ph RPA, we have two kinds of variations $\delta \mathrm{Q}_\omega|0\rangle$, namely $a^{\dagger}_m a_i|0\rangle$ and $a^{\dagger}_i a_m|0\rangle$, they are both-like gives two set of the equation of motion[4−5]

$$\begin{aligned} \langle \mathrm{RPA}|[a^{\dagger}_i a_m, [H, Q^{\dagger}_\omega]]|\mathrm{RPA}\rangle &= \hbar\Omega_\omega \langle \mathrm{RPA}|[a^{\dagger}_i a_m, Q^{\dagger}_\omega]|\mathrm{RPA}\rangle \,, \\ \langle \mathrm{RPA}|[a^{\dagger}_m a_i, [H, Q^{\dagger}_\omega]]|\mathrm{RPA}\rangle &= \hbar\Omega_\omega \langle \mathrm{RPA}|[a^{\dagger}_m a_i, Q^{\dagger}_\omega]|\mathrm{RPA}\rangle \,, \end{aligned} \tag{3}$$

where $\hbar\Omega_\omega$ is the excitation energy. If we assume that the correlated ground state does not differ very much from HF ground state, all expectation values in the HF approximation can be calculated, for example,[4−6]

$$\begin{aligned} \langle \mathrm{RPA}|[a^{\dagger}_i a_m, a^{\dagger}_n a_j]|\mathrm{RPA}\rangle &= \delta_{ij}\delta_{mn} - \delta_{mn}\langle \mathrm{RPA}|a_j a^{\dagger}_i|\mathrm{RPA}\rangle - \delta_{ij}\langle \mathrm{RPA}|a^{\dagger}_n a_m|\mathrm{RPA}\rangle \\ &\cong \langle \mathrm{HF}|[a^{\dagger}_i a_m, a^{\dagger}_n a_j]|\mathrm{HF}\rangle = \delta_{ij}\delta_{mn} \,. \end{aligned} \tag{4}$$

The probability of finding the particle-hole states $a^{\dagger}_m a_i|0\rangle$ and $a^{\dagger}_i a_m|0\rangle$ in the excited state $|\omega\rangle$ gives the amplitudes X_{mi} and Y_{im}

$$\langle 0|a^{\dagger}_i a_m|\omega\rangle \cong \langle \mathrm{HF}|[a^{\dagger}_i a_m, Q^{\dagger}_\omega]|\mathrm{HF}\rangle = X_{mi}, \quad \langle 0|a^{\dagger}_m a_i|\omega\rangle \cong \langle \mathrm{HF}|[a^{\dagger}_m a_i, Q^{\dagger}_\omega]|HF\rangle = Y_{mi} \,. \tag{5}$$

Equation (3) can be written in a compact matrix form,[4]

$$\begin{pmatrix} A & B \\ B^* & A^* \end{pmatrix} \begin{pmatrix} X \\ Y \end{pmatrix} = \hbar\Omega_\omega \begin{pmatrix} 1 & 0 \\ 0 & -1 \end{pmatrix} \begin{pmatrix} X \\ Y \end{pmatrix} , \tag{6}$$

with

$$\begin{aligned} A^{JT}_{minj} &= \langle \mathrm{HF}|[a^{\dagger}_i a_m, [H, a^{\dagger}_n a_j]]|\mathrm{HF}\rangle = (\varepsilon_m - \varepsilon_i)\delta_{mn}\delta_{ij} + V^{JT}_{mjin} \,, \\ B^{JT}_{minj} &= -\langle \mathrm{HF}|[a^{\dagger}_i a_m, [H, a^{\dagger}_j a_n]]|\mathrm{HF}\rangle = V^{JT}_{mnij} \,, \end{aligned} \tag{7}$$

ε_m is the single particle energy. In the JT couples scheme calculations, all the two-particle interaction matrices should be in particle-hole channel,[6]

$$V^{JT}_{mjin} = -\sum_{J'\,T'} (2J'+1)(2T'+1) \begin{Bmatrix} j_m & j_n & J' \\ j_i & j_j & J \end{Bmatrix} \begin{Bmatrix} 1/2 & 1/2 & T' \\ 1/2 & 1/2 & T \end{Bmatrix} V^{J'\,T'}_{mnij} \,. \tag{8}$$

The non-symmetric matrix (6) can be reduced to the diagonalization of a real symmetric matrix of half the dimension. Then, the matrices $(A \pm B)$ are real and symmetric. Let us assume that $(A - B)$ is positive-definite. Then it can be factorized as

$$(A - B) = LL^{\mathrm{T}}, \tag{9}$$

where L a lower-triangular real matrix and L^{T} its transpose. This is the square-root or Cholesky decomposition of the matrix.[25] Then the ph RPA matrix is left to real symmetric eigenvalue problem.[4]

$$L(A + B)L^{\mathrm{T}}R = \hbar^2\Omega_\omega^2 R\,. \tag{10}$$

Its solution gives the eigenvalues $\hbar^2\Omega_\omega^2$ and the normalized eigenvectors (amplitudes) R. Finally, the vectors X and Y can be recovered.

$$\begin{pmatrix} X \\ Y \end{pmatrix} = \frac{1}{2}[(\hbar\Omega_\omega)^{-1/2}L^{\mathrm{T}} \pm (\hbar\Omega_\omega)^{1/2}L^{-1}]R\,. \tag{11}$$

The RPA particle and hole occupation numbers can be calculated by using, for example, the number operator method[26−27] and one gets

$$\begin{aligned} n_p &= \sum_{hw} Y_{ph}^{\omega *}\, Y_{ph}^{\omega} - \frac{1}{2}\sum_{hp'h'}\sum_{ww'} Y_{ph}^{\omega *}\, X_{p'h'}^{\omega *}\, X_{p'h'}^{\omega'}\, Y_{ph}^{\omega'}\,, \\ n_h &= 1 - \sum_{p\nu} Y_{ph}^{\omega *}\, Y_{ph}^{\omega} \\ &\quad - \frac{1}{2}\sum_{ph'p'}\sum_{ww'} Y_{ph}^{\omega *}\, X_{p'h'}^{\omega *}\, X_{p'h'}^{\omega'}\, Y_{ph}^{\omega'}\,. \end{aligned} \tag{12}$$

2.2 *Electron Scattering*

Electron scattering form factor involving the angular momentum J and the momentum transfer q, between the initial and final nuclear shell model states of spin $J_{i,f}$ and isospin $T_{i,f}$ are[28]

$$\begin{aligned} |F_J^\eta(q)|^2 = \frac{4\pi}{Z^2(2J_i+1)}\Big| \sum_{T=0}^{1} \begin{pmatrix} T_f & T & T_i \\ -T_z & 0 & T_z \end{pmatrix} \\ \times \langle J_f T_f \|\hat{\mathcal{O}}_{JT}^\eta(q)\| J_i T_i\rangle F_{\mathrm{cm}}(q) F_{\mathrm{fs}}(q)\Big|^2, \end{aligned} \tag{13}$$

with η selecting the longitudinal (L), Coulomb (C), transverse electric (El) and transverse magnetic (Ma) form factors, respectively. $T_Z = (Z - N)/2$ is the projection of the total isospin. The nucleon finite size (fs) form factor is $F_{\mathrm{fs}}(q) = \exp(-0.43q^2/4)$ and $F_{\mathrm{cm}}(q) = \exp(q^2b^2/4A)$ is the correction for the lack of translational invariance in the shell model (center of mass correction), where A is the mass number and b is the harmonic oscillator size parameter.

The reduced matrix element of a one-particle operator between multi-particle states can be expressed as a sum of the product of the elements of multi-particle transition amplitudes times the single-particle matrix elements,

$$\langle J_f T_f \|\hat{\mathcal{O}}_{JT}^\eta(q)\| J_i T_i\rangle = \sum_{\mathrm{ph}} R_{\mathrm{ph}}^{JT} \langle p\|\hat{\mathcal{O}}_{JT}^\eta(q)\|h\rangle\,. \tag{14}$$

The reduced single particle matrix elements is[10]

$$\begin{aligned} \langle p\|\hat{\mathcal{O}}_{JT}^\eta(q)\|h\rangle = \sqrt{\frac{2T+1}{2}}\sum_{t_z} I_T(t_z) \\ \times \langle p\|\hat{\mathcal{O}}_{Jt_z}^\eta(q)\|h\rangle\,, \end{aligned} \tag{15}$$

with

$$I_T(t_z) = \begin{cases} 1, & \text{for } T = 0\,, \\ (-1)^{1/2-t_z}, & \text{for } T = 1\,, \end{cases}$$

and $t_z = 1/2(-1/2)$ a proton (a neutron).

The total longitudinal (L) and transverse (T) form factors are given by

$$|F^L(q)|^2 = \sum_{J\geq 0} |F_J^C(q)|^2, \tag{16}$$

$$|F^T(q)|^2 = \sum_{J=0} \{|F_J^{\mathrm{El}}(q)|^2 + |F_J^{\mathrm{Ma}}(q)|^2\}\,. \tag{17}$$

The total form factor is the sum of the longitudinal and transverse terms:

$$|F(q)|^2 = |F^L(q)|^2 + [1/2 + \tan^2(\theta/2)]|F^T(q)|^2, \tag{18}$$

where θ is the electron scattering angle and the parity of transition determined as,

$$\Delta\pi^{\mathrm{El}} = (-1)^J, \quad \Delta\pi^{\mathrm{Ma}} = (-1)^{J+1}\,. \tag{19}$$

The multipole operators in terms of single nucleon Pauli-isospin t_z are[29−30]

$$\hat{\mathcal{O}}_{JMt_z}^C(q) = \int \mathcal{M}_{JM}(\vec{r}, q)\cdot\rho(\vec{r}, t_z)\,\mathrm{d}\vec{r}, \tag{20}$$

$$\hat{\mathcal{O}}_{JMt_z}^{\mathrm{Ma}}(q) = \int \{\vec{\mathcal{M}}_{JJM}(\vec{r}, q)\cdot\vec{J}_c(\vec{r}, t_z) + [\vec{\nabla}\times\vec{\mathcal{M}}_{JJM}(\vec{r}, q)]\cdot\vec{\mu}(\vec{r}, t_z)\}\,\mathrm{d}\vec{r}, \tag{21}$$

$$\hat{\mathcal{O}}_{JMt_z}^{\mathrm{El}}(q) = \frac{1}{q}\int \{[\vec{\nabla}\times\vec{\mathcal{M}}_{JJM}(\vec{r}, q)]\cdot\vec{J}_c(\vec{r}, t_z) + q^2\vec{\mathcal{M}}_{JJM}(\vec{r}, q)\cdot\vec{\mu}(\vec{r}, t_z)\}\,\mathrm{d}\vec{r}, \tag{22}$$

where ρ is the charge density, $\vec{J}_c$ is the convection current coming from the intrinsic magnetic moments of target nucleus, and $\vec{\mu}(\vec{r})$ is the magnetization density operator obtained from magnetic current $\vec{J}_m = \vec{\nabla}\times\vec{\mu}$.

Scalar function $\mathcal{M}_{JM}(\vec{r}, q)$ is expressed in terms of the spherical Bessel function $\mathrm{j}_J(qr)$ and the spherical harmonic $\mathrm{Y}_{JM}(\Omega_r)$,

$$\mathcal{M}_{JM}(\vec{r}, q) = \mathrm{j}_J(qr)\mathrm{Y}_{JM}(\Omega_r)\,, \tag{23}$$

and vector function $\vec{\mathcal{M}}_{J'JM}(\vec{r},q)$ is expressed as,

$$\vec{\mathcal{M}}_{J'JM}(\vec{r},q) = \mathrm{j}_{J'}(qr)\vec{\mathrm{Y}}_{J'JM}(\Omega_r)\,, \tag{24}$$

the vector spherical harmonic $\vec{\mathrm{Y}}^{M}_{J'J}(\Omega_r)$, defined as,

$$\vec{\mathrm{Y}}_{J'JM}(\Omega_r) = \sum_{M',q}\langle J'M'lq|J\,M\rangle \mathrm{Y}_{J'M'}(\theta,\varphi)\hat{e}_q\,, \tag{25}$$

where

$$\left.\begin{aligned}\hat{e}_{\pm1} &= \mp\tfrac{1}{\sqrt{2}}(\hat{x}\pm \mathrm{i}\hat{y})\,,\\ \hat{e}_0 &= \hat{z}\,.\end{aligned}\right\} \tag{26}$$

The matrix elements for the required electron scattering operators used in this work are those of Brown *et al.*[31] In terms of these matrix elements, the reduced transition strength is given by[23]

$$B(\eta J,\ i\to f) = \frac{Z^2}{4\pi}\Big[\frac{(2J+1)!!}{k^J}\Big]^2|F^{\eta}_J(k)|^2, \tag{27}$$

where $k = E_x/\hbar c$.

3 Results and Calculations

The nuclear structure of ^{16}O nucleus is studied in the framework of ph RPA. The Hamiltonian is diagonalized in the model space $1p_{3/2}$, $1p_{1/2}$, $1d_{5/2}$, $1d_{3/2}$, and $2s_{1/2}$ in the presence of the WBP interaction.[24] Spurious center-of-mass- motion is removed by the usual method[32] of adding a center-of-mass Hamiltoian H_{CM} to the interaction.

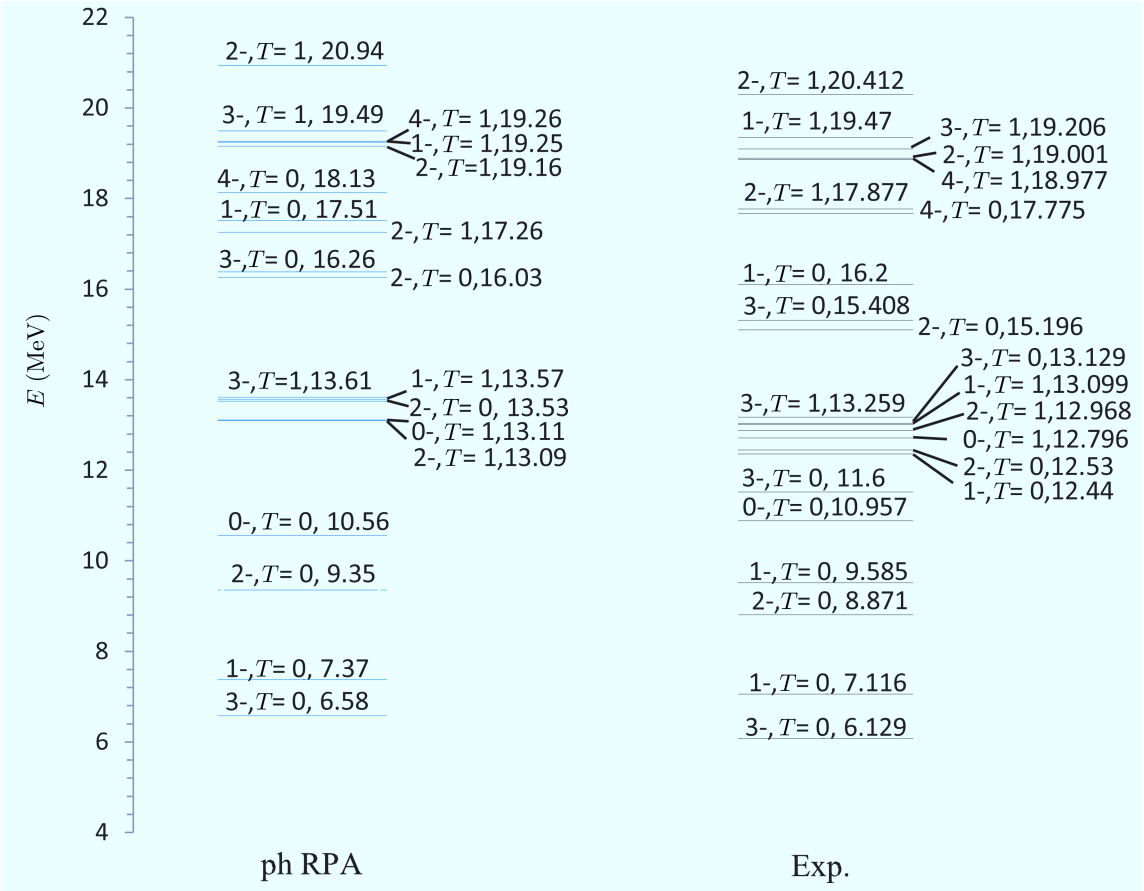

Fig. 1 The energy levels spectrum of ^{16}O for the ph RPA calculations compared to experiment.

Figure 1 gives the energy levels scheme for ^{16}O, generally it shows the computed states with the ph RPA have a good agreement with the experimental data. For example, the 1$^{\mathrm{st}}$ isoscalar ($T = 0$) 3^-, 1^-, 2^-, 0^- excited states occurs experimentally at 6.129, 7.116, 8.871, and 10.957 MeV respectively, with the ph RPA these states are found at 6.58, 7.37, 9.35, and 10.56 MeV. The four lowest isovector ($T = 1$) 2^- states occurs at 12.968, 17.877, 19.001, and 20.412 MeV in very good agreement with the calculated values: 13.09, 17.26, 19.16, and 20.94 MeV.

The occupation probabilities calculated in ph RPA for the single particle and hole orbits are represented in terms of bars in Fig. 2. The deviation from HF values ($n_p = 0$ and $n_h = 1$) means that the ground of ^{16}O is correlated.

The results of electron scattering form factors for the states: 1^-, $T = 0$ (7.116 MeV); 2^-, $T = 1$ (12.968 MeV); 2^-, $T = 1$ (20.412 MeV); and 3^-, $T = 0$ (6.129 MeV) are interpreted in terms of effective charges and the harmonic-

oscillator (HO) wave functions of size parameter b which is set to the value $b_{\rm rms}$ that reproduces the experimental root-mean square (rms) charge radius of ^{16}O.[33] Comparisons with the available experimental data are presented.

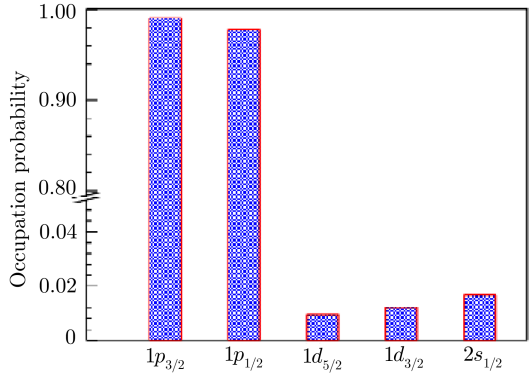

Fig. 2 Occupation probability of ^{16}O obtained by ph RPA calculations.

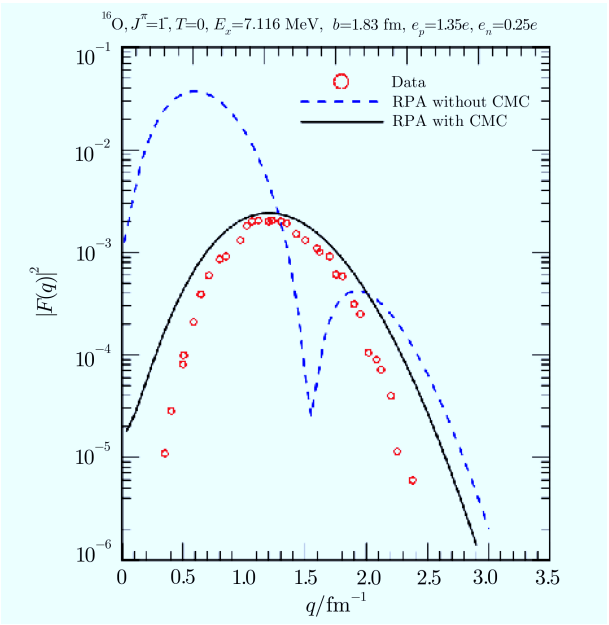

Fig. 3 The total form factor for the lowest energy level 1^-, $T = 0$ (7.116 MeV) of ^{16}O without center of mass correction (CMC) displayed as a dashed line and with CMC displayed as solid line in comparison with the experimental data of Ref. [33].

The selection rules conclude both electric $E1$ and Coulomb $C1$ dipole transitions contribute to the scattering of the lowest experimental 1^-, $T = 0$ (7.116 MeV) state. The total form factor calculated with both the ph RPA without CM correction (CMC) and the ph RPA with CMC are displayed in Fig. 3 in comparison with the experimental data.[33] Effective charges $e_p = 1.35e$ for proton and $e_n = 0.25e$ for neutron are used. The radial wave functions for the single-particle matrix elements are calculated with the HO-potential with the size parameter $b = 1.83$ fm.

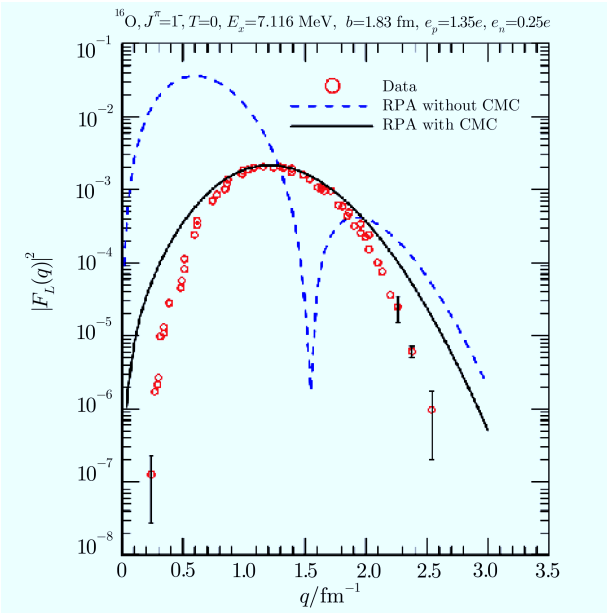

Fig. 4 The longitudinal form factor for the lowest energy level 1^-, $T = 0$ (7.116 MeV) of ^{16}O without center of mass correction (CMC) displayed as a dashed line and with CMC appears as solid line in comparison with the experimental data of Ref. [33].

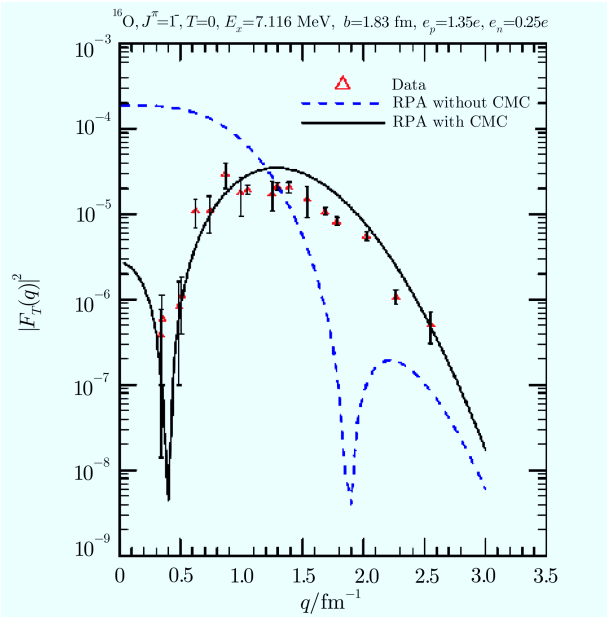

Fig. 5 The transverse form factor for the lowest energy level 1^-, $T = 0$ (7.116 MeV) of ^{16}O without center of mass correction (CMC) displayed as a dashed line with CMC appears as solid line in comparison with the experimental data of Ref. [33].

The calculated longitudinal form factors of ph RPA without CMC (dashed curve) and with CMC (solid curve) are shown in Fig. 4. The calculated ph RPA without CMC curve is far from experimental curve.[33] The calculated ph RPA with CMC curve seems as a close one to experimen-

tal data, especially around the peak of the form factor projected at $q \cong 1.3$ fm^{-1}.

The transverse form factors for this state are shown in Fig. 5. The ph RPA without CMC curve has a deformed shape (dashed line) and it is far from the experimental data,[33] which probably contain spurious states. The experimental data are very well explained with the ph RPA with CMC as shown by the solid line.

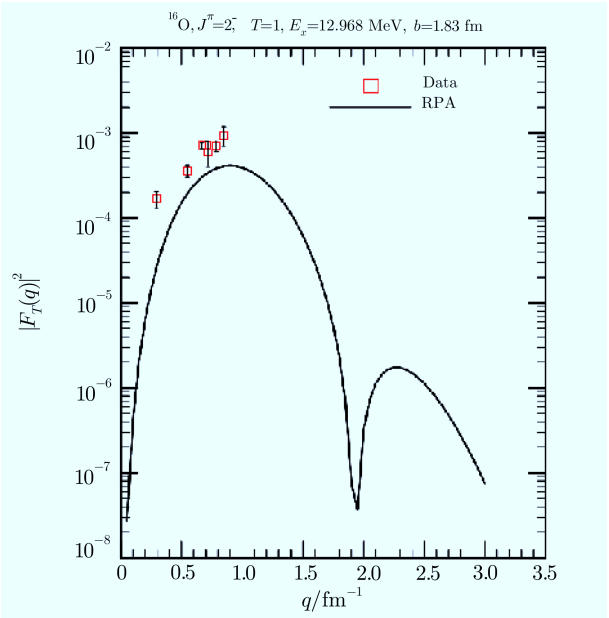

Fig. 6 The transverse $M2$ form factor for the lowest energy level 2^-, $T = 1$ (12.968 MeV) of ^{16}O in comparison with the experimental data of Ref. [34].

The second experimental excited state of 2^-, $T = 1$ was found at 20.412 MeV. Our ph RPA calculation predicts the value 20.94 MeV. The selection rules conclude only magnetic quadrupole M2 contributes to the scattering. The total form factor is shown in Fig. 7 as solid curve; it is somewhat over estimate with the available experimental.[35]

The selection rules conclude both Coulomb $C3$ and electric $E3$ transitions contribute to the scattering to 3^-, $T = 0$ (6.129 MeV) state. The longitudinal form factor calculated with ph RPA, displayed in Fig. 8 in comparison with the experimental data. Effective charges $e_p = 1.35e$ for proton and $e_n = 0.25e$ for neutron are used. The radial wave functions for the single-particle matrix elements are calculated with the HO-potential with the size parameter $b = 1.83$ fm. The calculations are very close to the experimental data.[33]

The magnetic quadrupole M2 transition according to selection rules contributes to the scattering to the lowest 2^-, $T = 1$ (12.968 MeV) state. The transverse form factor is calculated and displayed as solid curve in Fig. 6 in comparison with the experimental data.[34] The radial wave functions for the single-particle matrix elements are calculated with the HO-potential with size parameter $b = 1.83$ fm. The transverse form factor calculation is somewhat under estimate with the available experimental data.

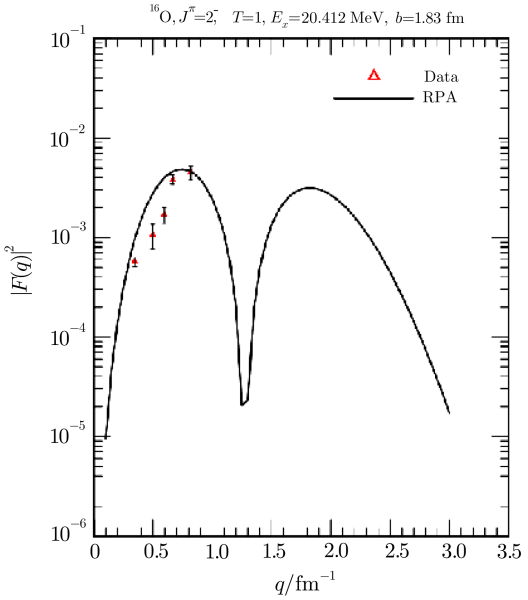

Fig. 7 The total form factor for the level 2^-, $T = 1$ (20.412 MeV) MeV of ^{16}O in comparison with the experimental data of Refs. [35].

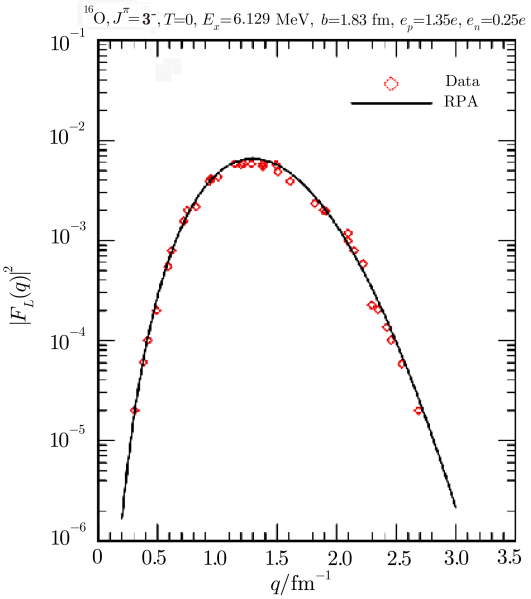

Fig. 8 The longitudinal form factor for the lowest energy level 3^-, $T = 0$ (6.129 MeV) of ^{16}O in comparison with the experimental data of Ref. [33].

Table 1 shows the comparison between the calculated and experimental values of the reduced transition strengths. The electromagnetic transitions within ph RPA framework to ground state expressed in Weisskopf units (W.u.). Our calculated results of B(M2),

$$2^-(12.968) \rightarrow 0^+(0.0)$$

and giant octupole resonance B(E3),

$$3^-(6.129) \rightarrow 0^+(0.0)$$

are in the same order as the experimental values. The giant dipole resonance B(E1),

$$1^-(7.116) \rightarrow 0^+(0.0)$$

is overestimate by a factor of about 100 compared with experimental value.

The discrepancy between the calculated and experimental B(E1) arises from kinematic sources. The harmonic oscillator single-particle wave functions are not defined relative to the center of mass of the nucleus, as they should be, but rather from the origin of a fixed external coordinate system. This gives rise to unphysical, or spurious, center-of-mass contributions to computed nuclear observables. The consequences are particularly serious for the electric dipole operator.[4−5,36] The simplest recipe to remove the spurious center-of-mass contributions, on the average, is to adopt the effective charges $e_p = 0.5e$ and $e_n = -0.5e$, or introducing isospin mixing within ph RPA Matrix using the proton and neutron single-particle energies.[36]

Table 1 Reduced transition strengths of ^{16}O.

Transition	Calculated (W.u.)	Experiment (W.u.)
B($E1$), $1^-(7.116) \rightarrow 0^+(0.0)$	1.40×10^{-2}	3.5×10^{-4}
B($M2$), $2^-(12.968) \rightarrow 0^+(0.0)$	5.68	1.0
B($E3$), $3^-(6.129) \rightarrow 0^+(0.0)$	10.96	1.35

4 Conclusions

The structure of closed-shell nucleus ^{16}O was studied in the framework of the ph RPA using Warburton and Brown interaction WBP, spurious center-of-mass-motion is removed by adding a center-of-mass Hamiltoian $H_{\rm CM}$ to the interaction. According to the results, a number of conclusions can be extracted; the spurious state of 1^- excitation is removed by adding a center-of-mass Hamiltoian $H_{\rm CM}$ to the interaction. Core polarization effects were also included through the effective charge, the calculated total, longitudinal and magnetic form factors with CMC for the lowest experimental 1^-, $T = 0$ (7.116 MeV) state agree well with the available experimental data. The harmonic oscillator single-particle wave functions are not defined relative to the center of mass of the nucleus therefore, B(E1) is overestimate by a factor of about 100 compared with experimental value.

The transverse M2 form factor for $1^{\rm st}$ 2^-, $T = 1$ (12.968 MeV) state calculation is somewhat under estimate agree with the available experimental data. The total form factor for the $4^{\rm th}$ 2^-, $T = 1$ (20.412 MeV) state is somewhat over estimate with the available experimental data. The longitudinal form factor for 3^-, $T = 0$ (6.129 MeV) state is very close to the data. The occupation probabilities for the single orbits are represented in terms of bars in Fig. 2. The deviation of the occupation probabilities of the single occupied and unoccupied states means that the ground of ^{16}O is correlated. Our calculated results of B(M2) and B(E3) are in the same order as the experimental values.

References

[1] M.F. De La Ripelle, S.A. Sofianos, and R.M. Adam, Ann. Phys. **316** (2004) 72.

[2] D.J. Rowe, Rev. Mod. Phys. **40** (1968) 153.

[3] E.M. De Guerra, *The Limits of the Mean Field*, *Lecture Notes in Physics*, Springer-Verlag, Berlin Heidelberg (2001).

[4] P. Ring and P. Schuck, *The Nuclear Many-Body Problem*, Springer-Verlag, New York (1980).

[5] D.J. Rowe, *Nuclear Collective Motion*, Butler & Tanner Ltd., London (1970).

[6] P.J. Brussaard and P.W. Glaudemans, *Shell Model Applications in Nuclear Spectroscopy*, North-Holland, Amsterdam (1977).

[7] F.A. Majeed and R.A. Radhi, Chin. Phys. Lett. **23** (2006) 2699.

[8] Ali. H. Taqi, Dirasat Journal-Pure Science-Jordon **33** (2006) 143.

[9] Ali. H. Taqi and R.A. Radhi, Turkish J. Phys. **31** (2007) 253.

[10] Ali. H. Taqi, Chin. J. Phys. **45** (2007) 530.

[11] T. Inakura, T. Nakatsukasa, and K. Yabana, Eur. Phys. J. A **42** (2009) 591.

[12] G. Colo, L. Cao, N.V. Giai, and L. Capelli, Comput. Phys. Commun. **184** (2013) 421.

[13] N. Paar, D. Vretenar, E. Khan, and G. Colo, Rep. Prog. Phys. **70** (2003) 691.

[14] D. Bianco, F. Knapp, N. Lo Iudice, P. Vesely, F. Andreozzi, G. De Gregorie, and Porrino, J. Phys. G: Nucl. Part Phys. **41** (2014) 025109.

[15] G. Giambrone, S. Scheit, F. Barranco, P.F. Bortignon, G. Colo, G.D. Sarchi, and E. Vigezzi, Nucl. Phys. A **726** (2003) 3.

[16] S. Péru and H. Goutte, Phys. Rev. C **77** (2008) 044313.

[17] N. Paar, P. Ring, T. Niksic, and D. Vretenar, Phys. Rev. C **67** (2003) 034312.

[18] H. Liang, N. Van Giai, and J. Meng, Phys. Rev. **101** (2008) 122502.

[19] M. Bender, P.H. Heenen, and P.G. Reinhard, Rev. Mod. Phys. **75** (2003) 121.

[20] R.A. Radhi, A.A. Abdullah, Z.A. Dakhil, and N.M. Adeeb, Nucl. Phys. A **696** (2001) 442.

[21] R.A. Radhi, Eur. Phys. J. A **34** (2007) 107.

[22] R. A. Radhi, A. A. Abdullah, and A. H. Raheem, Nucl. Phys. A **798** (2008) 16.

[23] R.A. Radhi and E.A. Salman, Nucl. Phys. A **806** (2008) 179.

[24] E.K. Warburton and B.A. Brwon, Phys. Rev. C **46** (1992) 923.

[25] W.H. Press, S.A. Teukolsky, W. Vetterling, and B. Flannery, *Numerical Recipes in Fortran: The Art of Scientific Computing*, Cambridge University Press, Cambridge (1997).

[26] D.J. Rowe, Phys. Rev. **175** (1968) 1283.

[27] F. Catara, G. Piccitto, M. Sambataro, and N. Van Giai, Phys. Rev. B **5** (1996) 536.

[28] T.W. Donnely and I. Sick, Rev. Mod. Phys. **56** (1984) 461.

[29] T. De Forest and J.D. Walecka, Adv. Phys. **15** (1966) 2.

[30] B.A. Brown, R.A. Radhi, and B.H. Wildenthal, Phys. Rep. **101** (1983) 313.

[31] B.A. Brwon, B.H. Wildenthal, C.F. Williamson, F.N. Rad, S. Kowalski, H. Crannell, and J.T. O'Berin, Phys. Rev. C **32** (1985) 1127.

[32] D.H. Glockner and R.D. Lawson, Phys. Lett. B **53** (1974) 313.

[33] T.N. Buti, J. Kelly, W. Bertozzi, *et al.*, Phys. Rev. C **33** (1986) 755.

[34] Vincent Gillet and N. Vinh Mau, Nucl. Phys. A **54** (1964) 312.

[35] T.E. Drake, E.L. Tomusiak, and H.S. Caplan, Nucl. Phys. A **118** (1968) 138.

[36] Jouni Suhonen, *from Nucleons to Nucleus*, Springer-Verlag, Berlin Heidelberg (2007).